

Iterative Detection and Decoding of Finite-Length Polar Codes in Gaussian Multiple Access Channels

Moustafa Ebada, Sebastian Cammerer, Ahmed Elkelesh, Marvin Geiselhart and Stephan ten Brink
 Institute of Telecommunications, Pfaffenwaldring 47, University of Stuttgart, 70569 Stuttgart, Germany
 {ebada,cammerer,elkelesh,geiselhart,tenbrink}@inue.uni-stuttgart.de

arXiv:2012.01075v2 [cs.IT] 3 Dec 2020

Abstract—We consider the usage of finite-length polar codes for the Gaussian multiple access channel (GMAC) with a finite number of users. Based on the interleave-division multiple-access (IDMA) concept, we implement an iterative detection and decoding non-orthogonal multiple access (NOMA) receiver that benefits from a low complexity, while scaling (almost) linearly with the amount of active users. We further show the conceptual simplicity of the belief propagation (BP)-based decoder in a step-by-step illustration of its construction. Beyond its conceptual simplicity, this approach benefits from an improved performance when compared to some recent work tackling the same problem, namely the setup of finite-length forward error-correction (FEC) codes for finite-number of users. We consider the 5th generation mobile communication (5G) polar code with a block length $N = 512$ applied to both a two-user and a four-user GMAC scenario with a sum-rate of $R_{\text{sum}} = 0.5$ and $R_{\text{sum}} = 1$, respectively. Simulation results show that a BP-based soft interference cancellation (SoIC) receiver outperforms a joint successive cancellation (JSC) scheme. Finally, we investigate the effect of a concatenated repetition code which suggests that alternative polar code design rules are required in multi-user scenarios.

I. INTRODUCTION

Polar codes [1] are not only proven to be capacity achieving when the block length tends to infinity, they also have shown to outperform low-density parity-check (LDPC) codes in the short-length regime [2]. A key feature of polar codes is their *per-bit-level* rate flexibility which can be seen as one of the reasons for their selection for the control channels of the 5G mobile communications standard [3]. Since their introduction, several decoding algorithms for polar codes have been developed. While successive cancellation list (SCL) decoding [4] is widely used, its inherent hard-decision output is limiting its application in iterative receiver architectures, such as iterative detection and demapping (IDD). Moreover, the serial nature of the algorithm puts limits to achievable latency and throughput. In contrast, iterative decoding schemes for polar codes such as BP [5] and its derivative [6] are based on the exchange of *soft* messages and, thus, appear more promising for iterative multi-user detection.

Driven by the continuous increase of active network devices, NOMA schemes have become a fast-growing field of research, opening up many exciting new research possibilities that require a careful reconsideration and re-evaluation of existing coding schemes [7]. For this, we focus on the application of short length communications motivated by IoT

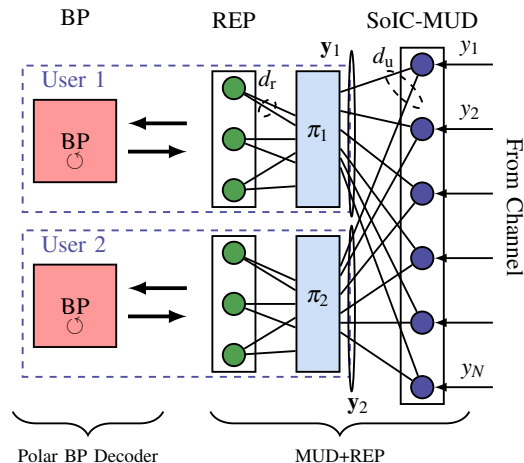


Fig. 1: Block diagram of a 2-user BP-based IDMA receiver.

sensor networks or similar industrial applications with strict latency requirements that prevent designers from using longer codewords. Note that, besides its conceptual simplicity in terms of orthogonalization of the channel resources, such a multi-user system may also significantly reduce the medium access latency. However, contrarily to the single-user case, the multi-user setup is characterized by many more code design parameters such as signal-to-noise-ratio (SNR), flexible number of users and, potentially, non-equal transmit powers that need to be considered for the optimal code design [8]. This amount of configurable system parameters – leading to the need of an individual code rate per user – renders a practical deployment difficult. In particular for the short length regime, it urges the need for a multi-user coding scheme with the highest possible rate flexibility while maintaining a powerful error-rate performance at low decoding complexity.

Polar codes were analytically shown to achieve the channel capacity region of the two-user binary input multiple access channel (MAC) [9], [10]. In [11], this was proven for the K-user scenario. However, none of these work provide an efficient decoding scheme for the case of finite code blocklength. The authors of [12] have proposed to use finite-length polar codes in an JSC-based IDD setup for two and four users for the special case of the unsourced MAC¹.

We adapt the well-known IDMA principle [13] to short

¹Unsourced MAC is a novel paradigm where the number of users, sharing the same codebook, can be unlimited; whereas only a finite number of users can be active on a time slot.

length polar codes with iterative decoding. IDMA is an attractive NOMA superposition coding scheme known to have an exceptionally good performance while maintaining a low decoding complexity using a simple multi-user detector (MUD) based on parallel interference cancellation (PIC). All users can transmit using the same channel code and modulation scheme, only a user-specific interleaver is required. We show that polar codes under iterative decoding can be seamlessly integrated into the *conventional* IDMA scheme by replacing the LDPC coding scheme. This promises an unseen rate flexibility on a *per-bit-level* and the full compatibility to the existing 5G polar coding framework. In this work, we focus on (relatively) short-length NOMA schemes that are difficult to realize with LDPC codes [8] due to their inherent random graph structure. Because of its inherent soft-in/soft-out (SISO) property, BP decoding of polar codes appears to be a promising candidate for iterative decoding and detection for multiple users allowing fully parallel decoding.

II. PRELIMINARIES

We provide a brief introduction to the IDMA system model and refer the interested reader to [8] for further details about the system setup.

A. IDMA System Model

Consider the IDMA system model with K_a active users, where each user encodes and decodes its data separately using a fixed polar code of code rate R_c followed by a repetition code of rate $R_r = \frac{1}{d_r}$. The total information rate is then given by $R_{\text{sum}} = K_a \cdot R_u$, where $R_u = R_c \cdot R_r$. After interleaving, the coded bits of the i^{th} user \mathbf{c}_i undergo a binary phase shift keying (BPSK) mapping to \mathbf{x}_i . Outputs from K_a active users are superimposed and transmitted over an additive white Gaussian noise (AWGN) channel which can be expressed as

$$\mathbf{y} = \sum_{i=1}^{K_a} \sqrt{P_i} \cdot \tilde{\mathbf{x}}_i + \mathbf{n} \quad (1)$$

where P_i is the received signal power of the i^{th} user, $\tilde{\mathbf{x}}_i = \mathbf{x}_i \cdot e^{j\varphi_i}$, with φ_i being random phase shifts which are independently and uniformly distributed in $[0, \pi)$ and user-specific. This phase scrambling was shown to improve the performance of superimposed multi-user scenarios [14], especially for AWGN channels.

B. Polar Codes

Polar codes are the first provably capacity-achieving channel codes over any arbitrary binary-input discrete memoryless channel [1]. Channel polarization is the core idea of polar codes, where synthesized bit-channels show a polarization behavior. The synthesized bit-channels polarize such that bit-channels become either noiseless or completely noisy and, thus, can be used for information/data transmission or frozen/known bit transmission. A polar code of length N and code dimension k (i.e., $\mathcal{P}(k, N)$) can be fully described with the frozen-bits set. Since every bit-channel can be either frozen or non-frozen, we can represent the frozen and non-frozen bits

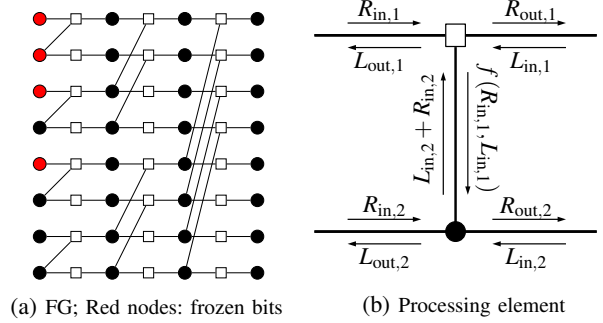


Fig. 2: Factor graph (FG) of a polar code with $N = 8$ and $R_c = 0.5$.

by a logical vector \mathbb{A} of length N . Element i in the \mathbb{A} -vector (i.e., a_i) indicates whether the i^{th} bit-channel is frozen or not. Throughout this work, $a_i = 0$ means that the i -th bit-channel is a frozen bit, while $a_i = 1$ indicates an information bit-channel. Thus, the polar code rate can be formulated as $R_c = \frac{k}{N} = \frac{\sum_{i=1}^N a_i}{N}$.

Originally, the choice of frozen/non-frozen bit-channels was based on the assumption of using a successive cancellation (SC) decoder to decode the polar code [1]. However, for finite length polar codes, the SC decoder performs poorly in terms of error-rate. Thus, other decoding algorithms were proposed in the literature (e.g., BP decoder [5] and SCL decoder [4]) outperforming the SC decoder. The BP decoder of polar codes is a soft-in/soft-out decoder, thus, it is very suitable for decoding concatenated coding schemes (e.g., see [15]–[17]) and suitable for iterative detection and decoding. In this work, we mainly focus on BP decoding of polar codes when applied to iterative detection and decoding.

C. BP Decoding and Factor Graphs

Polar codes can be visualized as a code on a graph [18] and, thus, iterative BP decoding (i.e., sum product algorithm (SPA)) can be used to decode polar codes [5]. The Forney-style factor graph of polar codes (shown in Fig. 2) consists of $\log_2(N)$ stages. Each stage contains $\frac{N}{2}$ processing elements (PEs) (shown in Fig. 2b). The channel output in terms of log-likelihood ratio (LLR) \mathbf{L}_{ch} is fed into the right-most stage of the factor graph. The code structure is defined by the left-most stage of the factor graph or, in other words, the frozen and non-frozen bit-channel positions. Then, LLR-based messages propagate over the edges of the factor graph from right-to-left (\mathbf{L} -messages) and then from left-to-right (\mathbf{R} -messages), until a maximum number of iterations $N_{\text{it,max}}$ is reached or until an early stopping condition is satisfied [19]. Throughout this work, we use a \mathbf{G} -matrix-based early stopping condition which terminates the iterations when $\hat{\mathbf{x}}$ is equal to $\hat{\mathbf{u}} \cdot \mathbf{G}$ where \mathbf{G} is the $k \times N$ polar code generator matrix. A codeword estimate $\hat{\mathbf{x}}$ and the information bits estimate $\hat{\mathbf{u}}$ are the outputs from the BP decoder after performing a hard-decision operation on the LLR messages in the right-most and the left-most stages, respectively.

The \mathbf{L} - and \mathbf{R} -messages are updated in each PE as follows:

$$R_{\text{out},1} = f(R_{\text{in},1}, L_{\text{in},2} + R_{\text{in},2})$$

$$R_{\text{out},2} = f(R_{\text{in},1}, L_{\text{in},1}) + R_{\text{in},2}$$

$$L_{\text{out},1} = f(L_{\text{in},1}, L_{\text{in},2} + R_{\text{in},2})$$

$$L_{\text{out},2} = f(R_{\text{in},1}, L_{\text{in},1}) + L_{\text{in},2}$$

where $f(L_1, L_2) = L_1 \boxplus L_2$ is commonly referred to as *boxplus* operator, which can be expressed as

$$f(x, y) = x \boxplus y = \log \frac{1 + e^{x+y}}{e^x + e^y}.$$

III. BP-BASED MULTI-USER DECODING AND DETECTION OF POLAR CODES

Similar to [8], the proposed decoder setup is composed of several blocks, namely:

- 1) a sub-optimal soft interference cancellation (SoIC)-based MUD block as mentioned before,
- 2) a repetition (REP) decoder,
- 3) a polar iterative decoder (i.e., BP decoder).

A. General scheme

Assume that \mathbf{y} is the received noisy channel observation of superimposed symbols \mathbf{x}_i . As depicted in Fig. 1, the proposed decoder setup processes \mathbf{y} as follows:

- 1) SoIC-MUD
 - Optimally: MUD would compute a posteriori probability (APP) per bit with complexity $\mathcal{O}(M^{K_a})$, where M is the number of constellation symbols per user
 - Here: a sub-optimal soft interference cancellation based low complexity MUD is implemented with complexity $\mathcal{O}(M \cdot K_a)$
 - $\hat{\mathbf{x}}_i$: feedback from single user decoder
 - \mathbf{y}_j : forward message after SoIC

$$\mathbf{y}_j = \mathbf{y} - \sum_{i \neq j} \hat{\mathbf{x}}_i$$

For more details, we refer the interested reader to [8].

- 2) Demapping and De-scrambling: where log-likelihood-ratio (LLR) of each bit is computed by the (soft) demapper while treating the residual interference as noise; followed by user-specific phase scrambling.
- 3) Deinterleaving: according to each user's specific interleaving pattern. Accordingly, the a priori knowledge of the REP decoder comes from the extrinsic message from MUD.
- 4) REP decoding: of code rate $R_r = \frac{1}{d_r}$ in case of repetition (discussed later), which enhances the signal-to-interference-plus-noise ratio (SINR) for further outer decoding. The extrinsic information of the j^{th} information symbol of the repetition code is the summation of the LLRs of all corresponding repeated symbols.
- 5) BP decoding: run a few $N_{\text{it,BP}}$ decoder-internal BP iterations (e.g., 1 or 2 iterations) to get an enhanced soft estimate of a codeword. As discussed later, more (sufficient) BP iterations are required in case of resetting

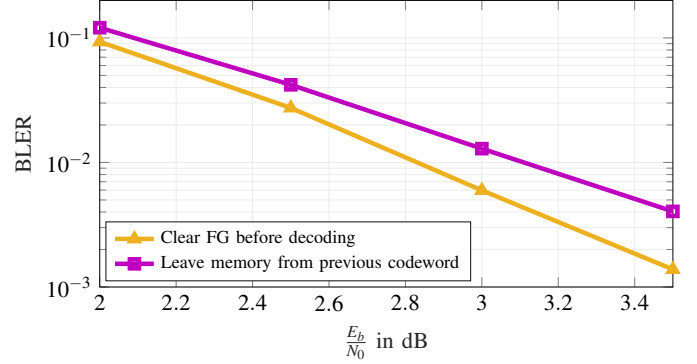


Fig. 3: Influence of initialization of the BP factor graph for a $\mathcal{P}(N = 512, k = 256)$ 5G polar code; 20 BP iterations; single user scenario.

the BP graph's internal memory after each BP decoding step.

- 6) Repetition
- 7) Interleaving
- 6) Scrambling and remapping
- 8) Repeating previous steps for $N_{\text{it,MUD}}$ times, and, thus, denoted as: $(N_{\text{it,BP}} \times N_{\text{it,MUD}})$.

Each individual BP decoder for a single user generates an improved soft-information output, which is then used by other user detectors to further de-noise the soft input to their BP decoders. The decoder setup is illustrated in Fig. 1.

B. Internal memory effects of polar BP factor graph

Internal LLR values of a BP factor graph instance, namely $L_{i,j}$ and $R_{i,j}$, are equivalently noted as *factor graph internal states*. These states form the so-called "internal memory" of a graph which affects the decoding convergence to a specific codeword. To further illustrate that, two BP decoding setups are compared in Fig. 3:

- 1) A BP decoding graph that clears the graph internal states before starting to decode a new codeword (i.e., resets the factor graph).
- 2) BP decoding graph where the internal memory of it persists (i.e., internal LLR values from previous codeword are not removed while decoding a new codeword).

As can be seen in Fig. 3, the *graph internal memory initialization* plays a significant role in the convergence behavior of a specific decoding instance. This has a strong impact on the multi user turbo decoder setup. After each MUD iteration, the BP factor graph is already at some state and, thus, the soft information is strongly affected by the previously acquired graph state. Thus, one solution might be as follows:

- 1) run BP for a sufficient number of iterations, instead of only a few iterations
- 2) pass information to MUD
- 3) reset BP factor graph (resetFG), i.e., "start over" whenever MUD output is updated.

The resultant new decoding setup enjoys an improved error-rate performance when compared to the previously mentioned setups, as depicted in Fig. 4 and Fig. 5.

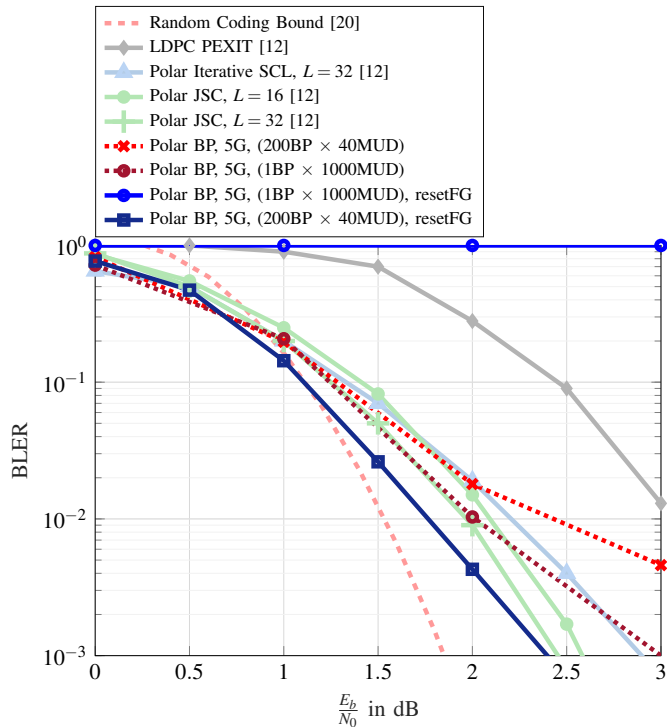


Fig. 4: BLER performance for codeword length $N = 512$ and $R_{\text{sum}} = 0.5$ bits per channel use with $K_a = 2$ users over an AWGN channel.

IV. RESULTS

Throughout this work, all polar BP curves correspond to a polar code of length $N = 512$ designed with the 5G bit-channel ordering [3], whereas the curves from [12] are optimized for their respective scheme (i.e., different polar code or \mathbb{A} -vector). We show results for two specific scenarios while benchmarking against the iterative SCL and JSC results of [12].

A. 2-User GMAC

Here, codewords from two active users are superimposed, each with a rate of $R_c = \frac{1}{4}$ and $d_r = 1$ (no repetition), thus, overall information rate $R_{\text{sum}} = \frac{1}{2}$. The error-rate simulation results for this setup are shown in Fig. 4.

B. 4-User GMAC

Here, codewords from four active users are superimposed with $R_{\text{sum}} = 1$ fixed. For the case of $R_c = \frac{1}{4}$ with $d_r = 1$ (no repetition) and $R_c = \frac{1}{2}$ with $d_r = 2$ (two-fold repetition). The error-rate simulation results for this setup are shown in Fig. 5.

Combined with repetition coding, the resultant scheme can be of significantly superior performance under joint polar BP-REP-SoIC decoding compared to that under JSC decoding introduced in [12]. It is worth-mentioning that scaling up the setup for (much) more users is straightforward.

V. THE REPETITION CODING Dilemma

It is a well-known fact that repetition coding has no coding gain for the single-user case. However, it seems as if repetition codes are very efficient for interference cancellation as pointed out in [8]. As depicted in Fig. 5, a joint BP-based IDD receiver

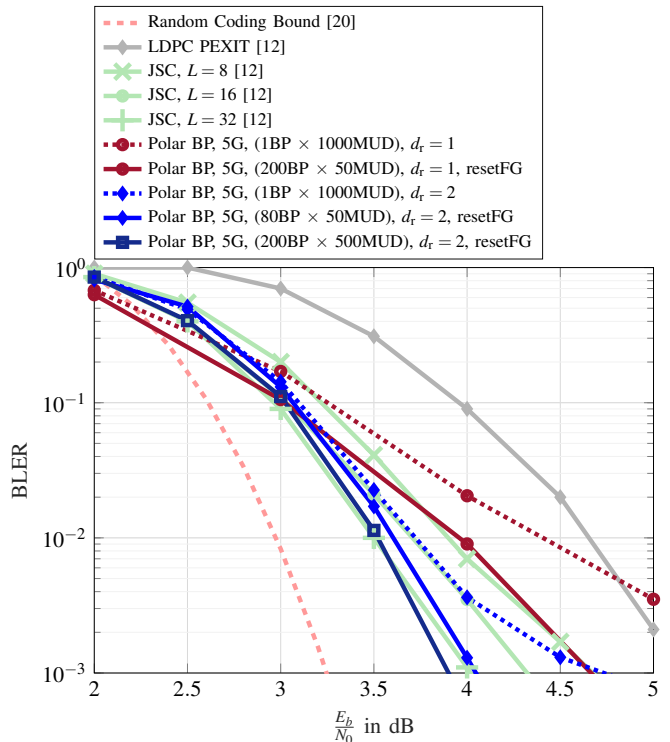


Fig. 5: BLER performance for codeword length $N = 512$ and $R_{\text{sum}} = 1$ bits per channel use with $K_a = 4$ users over an AWGN channel.

can benefit from an inner repetition code of repetition factor $d_r = 2$ when compared to a setup that does not involve a repetition code. The resultant code/receiver setup outperforms all of the previously mentioned coding/joint-IDD setups, as can be observed in Fig. 5. Here, we further explore this for the case of $K_a = 4$ active users.

A polar code of length N concatenated with an *inner* repetition code of repetition factor d_r can be viewed as another *equivalent* polar code of length $N \cdot d_r$, as depicted in Fig. 6. As can be seen, the *equivalent* polar code in Fig. 6b is constructed by appending $N \cdot (d_r - 1)$ frozen bits to the *original* polar code in Fig. 6a. The equivalent polar code results in the same error-rate performance when compared to the original code setup, as depicted in Fig. 8 (i.e., compare \bullet and \blacksquare).

Based on that, one might deduce that the effect of concatenating an inner repetition code, with the polar code is equivalent to a design enhancement for polar codes for the multi user setup (i.e., a better \mathbb{A} -vector tailored to the multi-user scenario). The performance gain with repetition is not merely a result of increasing the codeword length by repetition, as can be observed from Fig. 8 (i.e., compare \blacktriangle and \blacksquare). Fig. 7 shows a frozen channel chart (FCC) [21] for each of the *equivalent* and *plain* polar codes of the same length. One can easily see that the new equivalent polar code differs in many bit-positions from a polar code that follows the single user construction rules (e.g., 5G and Bhattacharyya-based polar codes). The equivalent polar code is, thus, not suitable for a traditional single user setup where it leads to a severe performance loss, as can be seen in Fig. 8 (i.e., compare \blacksquare and \blacktriangle).

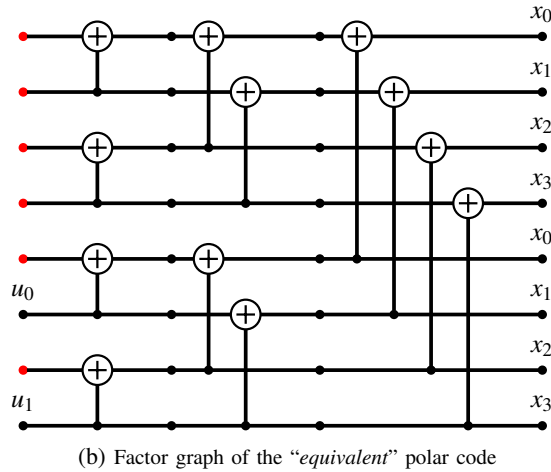
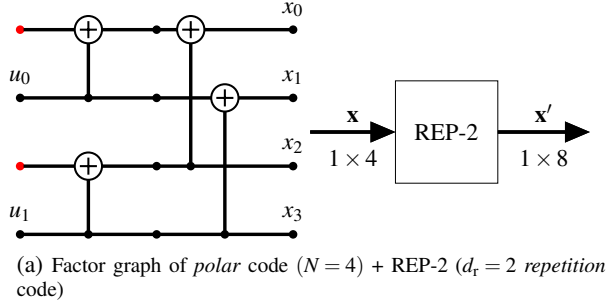


Fig. 6: An equivalent perspective of the polar code concatenated with an inner repetition code.

Polar code designed with Bhattacharyya for a BEC($\epsilon = 0.3172$) ($N = 1024$)



Polar code designed according to 5G specification ($N = 1024$)



Polar code ($N = 1024$) equivalent to polar code ($N = 512$) with 2-repetition



Fig. 7: Difference between the equivalent \mathbb{A} -vector and a good single-user code design (i.e., 5G-based \mathbb{A} -vector) visualized using a frozen channel chart (FCC) [21]. The 1024 bit positions are plotted over a 16×64 matrix. Note that the bit-channels are sorted with decreasing Bhattacharyya parameter value. White: non-frozen; colored: frozen.

VI. CONCLUSION

In this paper, we proposed the usage of BP decoders for iterative detection and decoding of polar codes in a multi-user scenario. Combined with repetition coding, the resulting

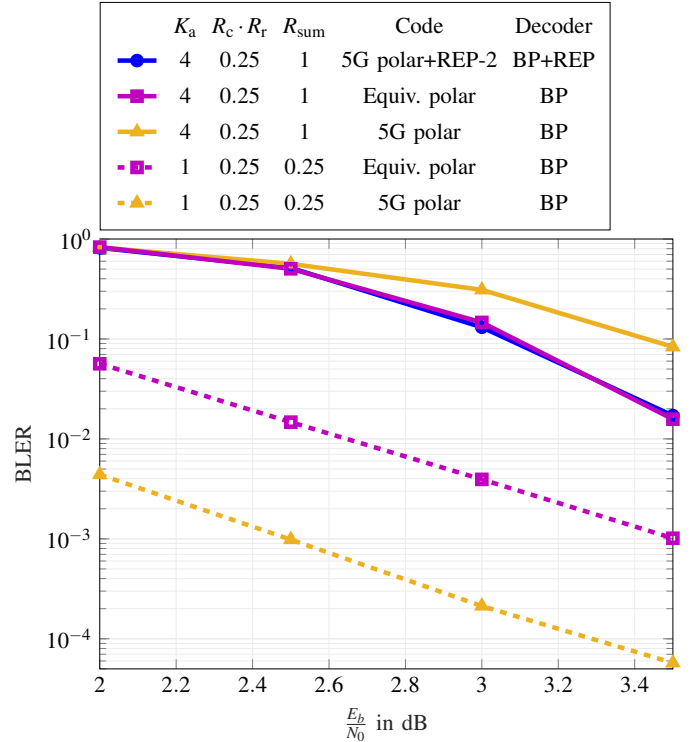


Fig. 8: Error-rate of a conventional polar code concatenated with an inner repetition code compared to that of the equivalent longer polar code, similar to Fig. 6. Single-user performance is also plotted to show difference to multi-user setup (i.e., in a multi-user setup: equivalent code is superior in performance to that of a typically constructed polar code without repetition; whereas for a single-user setup it is exactly the opposite). Sum-rates of both setups are obviously not comparable. All curves shown for codeword length $N = 1024$.

scheme can compete with, and even outperform, JSC based IDD [12] for two and four users, while the inherent parallel nature of polar BP decoding may lead to more desirable hardware implementations. Further analysis is required to investigate the case for a massive number of users.

We also shed some light on the gains by the usage of a concatenated repetition code and verified its effectiveness in Monte-Carlo simulations, a theoretical explanation remains, however, an open problem. We concluded that this repetition code corresponds to a different selection of frozen bit-positions (different \mathbb{A} -vector) in the polar code design, suggesting that the multi-user detection can benefit from a different polar code design than the single-user case. Finding such an optimized polar code construction is an interesting open future work and an important step towards efficient deployment of multi-user polar coding with iterative detection and decoding.

REFERENCES

- [1] E. Arkan, "Channel Polarization: A Method for Constructing Capacity-Achieving Codes for Symmetric Binary-Input Memoryless Channels," *IEEE Trans. Inf. Theory*, vol. 55, no. 7, pp. 3051–3073, Jul. 2009.
- [2] M. C. Coşkun, G. Durisi, T. Jerkovits, G. Liva, W. E. Ryan, B. Stein, and F. Steiner, "Efficient Error-Correcting Codes in the Short Blocklength Regime," *Physical Communication*, vol. 34, pp. 66–79, Jun. 2019.
- [3] "Technical Specification Group Radio Access Network," *3GPP, 2018, TS 38.212 V.15.1.1*. [Online]. Available: http://www.3gpp.org/ftp/Specs/archive/38_series/38.212/

- [4] I. Tal and A. Vardy, "List Decoding of Polar Codes," *IEEE Trans. Inf. Theory*, vol. 61, no. 5, pp. 2213–2226, May 2015.
- [5] E. Arıkan, "Polar Codes: A Pipelined Implementation," *Proc. 4th ISBC*, pp. 11–14, 2010.
- [6] A. Elkelesh, M. Ebada, S. Cammerer, and S. ten Brink, "Belief Propagation List Decoding of Polar Codes," *IEEE Commun. Lett.*, vol. 22, no. 8, pp. 1536–1539, Aug. 2018.
- [7] L. Dai, B. Wang, Z. Ding, Z. Wang, S. Chen, and L. Hanzo, "A Survey of Non-Orthogonal Multiple Access for 5G," *IEEE Commun. Surveys & Tutorials*, vol. 20, no. 3, pp. 2294–2323, 2018.
- [8] X. Wang, S. Cammerer, and S. ten Brink, "Near-Capacity Detection and Decoding: Code Design for Dynamic User Loads in Gaussian Multiple Access Channels," *IEEE Trans. Commun.*, vol. 67, no. 11, pp. 7417–7430, 2019.
- [9] E. Şaşođlu, E. Telatar, and E. M. Yeh, "Polar Codes for the Two-User Multiple-Access Channel," *IEEE Trans. Inf. Theory*, vol. 59, no. 10, pp. 6583–6592, 2013.
- [10] S. Öney, "Successive Cancellation Decoding of Polar Codes for the Two-User Binary-Input MAC," in *IEEE Inter. Symp. Inf. Theory (ISIT)*, 2013, pp. 1122–1126.
- [11] E. Abbe and E. Telatar, "Polar Codes for the m -User Multiple Access Channel," *IEEE Trans. Inf. Theory*, vol. 58, no. 8, pp. 5437–5448, 2012.
- [12] E. Marshakov, G. Balitskiy, K. Andreev, and A. Frolov, "A Polar Code Based Unsourced Random Access for the Gaussian MAC," in *IEEE 90th Vehicular Technology Conference (VTC2019-Fall)*, 2019, pp. 1–5.
- [13] Li Ping, Lihai Liu, Keying Wu, and W. K. Leung, "Interleave Division Multiple-Access," *IEEE Trans. on Wireless Commun.*, vol. 5, no. 4, pp. 938–947, 2006.
- [14] G. Song and J. Cheng, "Distance Enumerator Analysis for Interleave-Division Multi-User Codes," *IEEE Trans. Inf. Theory*, vol. 62, no. 7, pp. 4039–4053, 2016.
- [15] J. Guo, M. Qin, A. G. i Fàbregas, and P. H. Siegel, "Enhanced Belief Propagation Decoding of Polar Codes through Concatenation," in *IEEE Inter. Symp. Inf. Theory (ISIT)*, Jun. 2014, pp. 2987–2991.
- [16] A. Elkelesh, M. Ebada, S. Cammerer, and S. ten Brink, "Improving Belief Propagation Decoding of Polar Codes Using Scattered EXIT Charts," in *IEEE Inf. Theory Workshop (ITW)*, Sep. 2016, pp. 91–95.
- [17] —, "Flexible Length Polar Codes through Graph Based Augmentation," in *IEEE Inter. ITG Conf. on Syst., Commun. and Coding (SCC)*, Feb. 2017.
- [18] G. D. Forney, "Codes on Graphs: Normal Realizations," *IEEE Trans. Inf. Theory*, vol. 47, no. 2, pp. 520–548, Feb. 2001.
- [19] B. Yuan and K. K. Parhi, "Early Stopping Criteria for Energy-Efficient Low-Latency Belief-Propagation Polar Code Decoders," *IEEE Trans. Sig. Process.*, vol. 62, no. 24, pp. 6496–6506, Dec. 2014.
- [20] Y. Polyanskiy, "A Perspective on Massive Random-Access," in *IEEE Inter. Symp. Inf. Theory (ISIT)*, 2017, pp. 2523–2527.
- [21] A. Elkelesh, M. Ebada, S. Cammerer, and S. ten Brink, "Decoder-Tailored Polar Code Design Using the Genetic Algorithm," *IEEE Trans. Commun.*, vol. 67, no. 7, pp. 4521–4534, Jul. 2019.